Journal of Plant Pathology (2024) 106:1295–1309
https://doi.org/10.1007/s42161-024-01685-1

ORIGINAL ARTICLE

Control of coptis root rot by combination of *Bacillus cereus* isolate Y9 and other antagonistic microorganisms

Pengying Mei[1] · Tao Dou[1] · Xuhong Song[1] · Longyun Li[1]

Received: 31 August 2023 / Accepted: 29 May 2024 / Published online: 24 June 2024
© The Author(s) 2024

Abstract
Root rot is a destructive soil-borne disease of *Coptis chinensis*, which depends on chemical control at present, and more attention should be paid to biocontrol of disease. In the present research, isolate Y9 isolated from healthy root samples of *Coptis*, was identified as *Bacillus cereus.* Further screening and pot experiments showed that *B. cereus* isolate Y9 inhibited the growth of the main causal agents of coptis root rot disease (*Fusarium solani* and *F. avenaceum*) and seven other phytopathogenic fungi. The application of *B. cereus* isolate Y9 and compatible *Trichoderma harzianum*, *T. atroviride* and *B. amyloliquefaciens*, singly and in combination were found to be effective against *Fusarium* root rot in vitro and in field experiments. In field experiments, combinations of *T. harzianum* + *B. amyloliquefaciens* + Y9 (HYJ, in ratio of 1:1:1) showed the highest control efficacy of 63.85%, which was higher than the expected value (53.18%), indicating synergistic effect on the control of coptis root rot. Therefore, *B. cereus* isolate Y9 may be a potential biological control agent, and combined use with *T. harzianum* and *B. amyloquefaciens* offered even greater potential. The long-term effects of isolate *B. cereus* Y9 and its combinations on *C. chinensis* should be assessed in different locations and seasons in the future.

Keywords *Trichoderma* · *Bacillus amyloliquefaciens* · Synergistic effect · Multilocus phylogeny · Biocontrol

Introduction

Chinese goldthread (*Coptidis rhizoma*), a widely used traditional Chinese medicine, is the dried rhizome of *Coptis chinensis* Franch., *C. deltoidea* C. Y. Cheng et Hsiao or *C.teeta* Wall., commonly known as 'Wei-lian', 'Ya-lian' or 'Yun-lian', respectively (Commission 2020) (p. 177). The Shizhu county, Chongqing, produces morethan 60% of the Chinese goldthread, which has been exported to many countries and regions.The main medicinal active ingredients of Chinese goldthread are alkaloids, such as berberine, epiberberine, coptisine, palmatine chloride, columbamine, thaliotrine and jatrorrhizine. These alkaloid compounds are reported to have a wide range of pharmacological activities, such as antimicrobial activity, antiinflammatory, antiatherosclerotic, antidiabetic, antitumor effects, antiviral, dispelling dampness, and detoxification agents (Song et al. 2023). However, root rot significantly reduced the content of these alkaloids (except jatrorrhizine), thus seriously affecting the quality of Chinese goldthread (Song et al. 2023). Root rot is a severe soil-borne disease, and *Fusarium* spp. (Luo et al. 2014; Cheng et al. 2020; Wu et al. 2020; Mei et al. 2021b), *Diaporthe* spp. (Mei et al. 2021a), *Pythium* spp. (Wu et al. 2021b) and *Ilyonectria* spp. (Wu et al. 2021a) were reported as its causal agents. Among these, *F. solani* is the main pathogenic fungus, which is responsible for disease on about 100 genera of plants (Coleman et al. 2009).

As one of the most serious diseases in *Coptis*, the incidence rate of root rot can reach to 40%, leading to about 67% yield loss in Shizhu county (Mei et al. 2021b). Infected coptis plants showed stunted growth, and most of the fibrous and main roots were brown or showed black discoloration, while healthy roots were yellow. Severely infected plants were wilted and necrotic. The prevention and control of these diseases is largely achieved by applying chemical fungicides; however, due to the continuous improvement of public concern about drug safety, chemical residues and environmental pollution, the application of pesticides should be reduced to ensure the quality of the traditional Chinese medicine. Biological controls using beneficial

✉ Longyun Li
lilongyun8@163.com

[1] Chongqing Academy of Chinese Materia Medica, Chongqing 400065, China

microorganisms are an alternative way to minimize the pollution and chemical residues.

Biocontrol agents (BCAs), in particular *Bacillus* spp. have showed an antagonistic effect against a wide spectrum of diseases, and are used to control the phytopathogenic fungi, such as *Rhizoctonia solani*, *Botrytis cinerea*, *Verticillium dahliae*, *Sclerotinia sclerotiorum*, *Alternaria* spp., and *Fusarium* spp., in tomato (Gao et al. 2017; Zhao et al. 2022), pepper (Jiang et al. 2018), cotton (Hasan et al. 2020), cannabis (Balthazar et al. 2022), ginseng (Wei et al. 2023) and bean crops (Han et al. 2021; Hashem et al. 2021). *Trichoderma* spp. are also one of the most commonly used BCAs against a broad spectrum of root, shoot, and post-harvest pathogens (Zin and Badaluddin 2020; Poveda and Eugui 2022; Behiry et al. 2023). Considering the limitation of using a single biocontrol strain (Mazzola and Freilich 2017), application of strain mixtures in controlling soil-borne diseases has begun to be widely used in modern agriculture (Ma et al. 2022).

Combined use of *Trichoderma* and compatible *Bacillus* is possible to offer even greater potential as plant growth promoters and as biocontrol agents (Poveda and Eugui 2022). It was reported that the co-culture of *T. asperellum* GDFS1009 and *B. amyloliquefaciens* 1841 improved the maize and wheat growth and biocontrol activity (Karuppiah et al. 2019a, b). Similarly, mixed culture fermentation of *B. amyloliquefaciens* and *T. longibrachiatum* improved the biocontrol efficiency on tomato *Fusarium* wilt (Ma et al. 2022). Some researchers have studied the fungicide sensitivity of the causal agents and the ecological factors of coptis root rot (Cheng et al. 2020; Yang et al. 2020). An eight year rotation, combined with chemicals, such as metalaxyl·hymexazol 3% AS, can effectively control coptis root rot (Yang et al. 2020).

In China, the control of root rot disease of coptis is primarily based on the use of fungicides, which has resulted in chemical residues. Therefore, it is vital to explore for alternative strategies to manage these pathogens. However, the potential of biological agents for control has not been fully explored. Despite, the biocontrol mechanism of *Bacillus* spp. and *Trichoderma* spp. are different, and the combined application of *Bacillus* spp. and *Trichoderma* spp. is more effective than using a single strain in controlling soil-borne diseases. Hence, the present study aims to: (i) screen and identify beneficial microorganisms that have antagonistic and control effects on coptis root rot; (ii) assess the effectiveness of a new screened isolate against mycelial growth of the main causal agents of coptis root rot disease (*F. solani* and *F. avenaceum*); (iii) confirm its efficacy through pot test and field trials.

Materials and methods

Microorganisms

The Y9 bacterium was isolated from a healthy root sample of *Coptis chinensis* Franchet in Chongqing, China. The *Bacillus amyloliquefaciens* (CGMCC 1.15674) was obtained from China General Microbiological Culture Collection Center. The *B. subtilis* (ATCC 6633), *B. cereus* (CMCC(B) 63303) and *B. thuringiensis* (ATCC 10792) were obtained from Shanghai Luwei Technology Co., Ltd. The bacteria were maintained on nutrient agar (NA) medium. The *Trichoderma harzianum* T22 and *T. atroviride* T1 cultures were preserved in Chongqing Academy of Chinese Meteria Medica. The fungal pathogens *F. solani* and *F. avenaceum* causing root rot of *Coptis chinensis* were isolated from diseased roots, previously (Mei et al. 2021b). The fungi were maintained on potato dextrose agar (PDA) medium.

Phylogenetic analysis of *B. cereus* Y9

Genomic DNA of the isolate was extracted with TIANamp Bacteria DNA Kit (Tiangen, Beijing, China). The 16S rRNA gene was amplified with universal primers 27f and 1492r (Frank et al. 2008). Specific primers *gyrA*-f, *gyrA*-r and *rpoB*-f, *rpoB*-r were used for PCR analysis of the DNA gyrase subunit A (*gyrA*) and RNA polymerase beta subunit (*rpoB*) gene, respectively (Yan et al. 2022). The primer sequences that have been used for the amplification were listed in Table 1. The PCR mixture (50 µL) contained 1 µL of DNA template, 25 µL of 2×Hieff® Robust PCR Master Mix (Yeasen, Shanghai, China), 20 µL of ddH_2O, and 2 µL of each primer (10 µM). The PCR amplification was conducted in a thermal cycler (ABI ProFlex) according to the following protocol: initial denaturation at 95 °C for 5 min, followed by 35 cycles of denaturation at 95 °C for 10 s, annealing at 55 °C for 20 s, extension at 72 °C for 30 s, and a final extension at 72 °C for 5 min. The PCR product

Table 1 Primers used for bacterial identification

Primer name	Sequence (5′-3′)	Reference
27f	AGAGTTTGATCCTGGCTCAG	Frank et al. (2008)
1492r	TACCTTCTTACGACTT	
gyrA-f	GCGTCTGCAACGTTTAACTGG	Yan et al. (2022)
gyrA-r	TGTCGCTACCTCTTGCTCATC	
rpoB-f	ACAGAGCTTGGCGTTGAAGT	Yan et al. (2022)
rpoB-r	GCTTCTTGGCTGAATGAAGG	

was purified and sequencing was performed by the Sanger method (Tsingke Biotechnology Co., Ltd.). All sequences were deposited in the GenBank.

Sequences of the same genus for each gene were obtained from GenBank and multilocus phylogeny was reconstructed using PhyloSuite with the help of several plug-in programs (Zhang et al. 2020; Xiang et al. 2023): Three sequences were aligned in batches with MAFFT (Katoh and Standley 2013), then the alignments were refined with MACSE (Ranwez et al. 2018). Ambiguously aligned fragments of three alignments were removed in batches using trimAl (Capella-Gutiérrez et al. 2009). ModelFinder was used to select the best-fit partition model using BIC criterion (Kalyaanamoorthy et al. 2017). Bayesianinference phylogenies were inferred using MrBayes under partition model (200,000 generations, 1000 sampling freq, 0.25 burn-in fraction, default values for the other parameters) (Ronquist et al. 2012). When the average standard deviation of split frequencies falls below 0.01, stop the run and infer the tree. The posterior probability values were used to assess branch support.

The phenotypic and biochemical characteristics of *B. cereus* Y9

Main physiological and biochemical test was used to distinguish Y9, with the two standard strains (*B. cereus*, CMCC(B) 63303 and *B. thuringiensis*, ATCC 10792) as controls. Gram and endospore staining was performed according to the manufacturer's instructions for Gram stain kit and Spore stain kit (Solarbio, Beijing, China), respectively. Biochemical characterization (e.g. motility, citrate, catalase, Voges-Proskauer, methyl red, nitrate reduction and parasporal crystal) was conducted according to Systemic identification manual of common bacteria (Dong and Cai 2001) (pp. 353–384). The principal distinguishing characteristics of *B. cereus* and the related species were listed in Table 2. *B. thuringiensis* can produce the parasporal crystals which were different rhombus and small cuboidal, while *B. cereus* not.

Table 2 Physiological and biochemical characteristics of isolate Y9

Characteristics	*B. cereus*	*B. thuringiensis*	Y9
Motility	+	+	+
Catalase	+	+	+
Starch hydrolysis	+	+	+
Gelatinliquefaction	+	+	+
Egg yolk	+	+	+
Mannitol	–	–	–
Methyl red	+	+	+
Voges-Proskauer	+	+	+
Citrate	+	+	+
Nitrate reduction	+	+	+
Parasporal crystal	–	+	–

Compatibility among biocontrol agents

Bacillus and *Trichoderma* were tested for their compatibility among each other following the method described by Barbosa et al. (2018). To prepare the cell suspensions, two bacterial isolates were grown on NA for 24 h at 30 °C and then transferred to nutrient broth with shaking at 180 rpm at 30 °C for 12 h ($OD_{600}=0.5$, approximately 6×10^6 CFU mL^{-1}), while three fungi were routinely grown on PDA plates at 25 °C and spore suspensions were prepared by scraping the spores from seven-day-old plates (10^6 conidia mL^{-1}). The cell suspensions were streaked horizontally and vertically to each other on PDA and NA plates. The plates were incubated at 30 °C for 72 h and observed for the inhibition zone. Compatible isolates were able to grow over each other, while the presence of inhibition zone indicated the incompatibility. Three plates per replicate were analyzed, and all experiments were performed in triplicate.

The co-cultured combinations

The liquid BP broth (beef extract 0.3% and peptone 0.5%) was used in this study for both pure and co-cultivation (Wu et al. 2018). Two strains of *Trichoderma* spp. (*T. harzianum* T22 and *T. atroviride* T1) and two strains of *Bacillus* spp. (Y9 and *B. amyloliquefaciens* CGMCC 1.15674) were tested individually and in combination to assess the radial growth of *F. solani* and *F. avenaceum*, and the specific combinations with different inoculation ratios were listed in Table 3. Briefly, 1 mL of *T. harzianum* or *T. atroviride* inocula (10^6 conidia mL^{-1}) was pre-cultured for 48 h in 100 mL of BP broth, subsequently the corresponding amount of Y9 or *B. amyloliquefaciens* inocula ($OD_{600}=0.5$, approximately 6×10^6 CFU mL^{-1}) was inoculated into the preculture medium and incubated at 180 rpm at 30 °C for another 48 h (Karuppiah et al. 2019a). For pure culture, 1 mL of *Trichoderma* spp. or *Bacillus* spp. was singly inoculated into 100 mL of BP broth, incubated in shaker for 4 days.

Antifungal activity in vitro

The antagonistic activity of strain Y9 or the co-cultured combinations against the seven fungal pathogens (*F. oxysporum*, *F. graminearum*, *F. fujikuroi*, *Clonostachys rosea*, *Collteotrichum fructicola*, *Collteotrichum gloeosporiodies*, and *Pestalotiopsis olivacea*) were tested in a double culture assay as described previously (Han et al. 2022). A fungal disc (6 mm in diameter) or a 10-µL aliquot of spore suspension was placed in the center of PDA plate. Bacterial isolates were streaked 2 cm from the center where they crossed. Plates inoculated with fungal pathogens and sterile water were used as controls. Plates were incubated in the dark at

Table 3 Effects of microorganisms alone or in combination on mycelial growth of *F. solani* and *F. avenaceum*

No.	Treatments	Inoculation ratios (v / v)	*F. solani*		*F. avenaceum*	
			Mycelial growth (mm)	Inhibition rate (%)	Mycelial growth(mm)	Inhibition rate (%)
T0	Pathogen		47.03 ± 0.18^{a}		46.66 ± 0.58^{a}	
T1	*B. cereus* Y9		22.09 ± 0.61^{b}	51.60 ± 1.77^{d}	21.77 ± 0.20^{b}	54.03 ± 0.77^{c}
T2	*B. amyloliquefaciens*		22.88 ± 0.64^{b}	50.89 ± 2.06^{d}	24.33 ± 1.02^{b}	51.51 ± 1.91^{c}
T3	*T. harzianum*		16.15 ± 0.36^{ef}	65.63 ± 0.29^{ab}	15.50 ± 0.96^{de}	66.34 ± 1.51^{a}
T4	*T. atroviride*		16.70 ± 0.07^{d}	64.46 ± 0.06^{ab}	16.23 ± 0.07^{d}	64.83 ± 0.66^{a}
T5	*T. harzianum* + Y9	1:5	15.90 ± 0.23^{ef}	66.18 ± 0.22^{a}	15.44 ± 1.44^{de}	66.68 ± 3.35^{ab}
T6		1:2	16.16 ± 0.09^{e}	65.62 ± 0.12^{ab}	15.03 ± 0.97^{de}	67.04 ± 2.11^{a}
T7		1:1	15.71 ± 0.07^{ef}	66.58 ± 0.05^{a}	14.22 ± 1.04^{de}	68.52 ± 2.52^{a}
T8		2:1	16.18 ± 0.91^{def}	65.56 ± 1.93^{ab}	16.17 ± 2.22^{de}	65.51 ± 5.51^{abc}
T9		5:1	15.66 ± 0.12^{ef}	66.68 ± 0.08^{a}	15.49 ± 0.74^{de}	66.69 ± 1.22^{a}
T10	*T. atroviride* + Y9	1:5	18.43 ± 0.29^{c}	60.79 ± 0.49^{c}	14.59 ± 1.45^{de}	66.10 ± 4.29^{abc}
T11		1:2	23.31 ± 0.23^{b}	50.40 ± 0.41^{d}	18.51 ± 1.48^{cd}	57.01 ± 4.75^{abc}
T12		1:1	21.14 ± 0.99^{bc}	55.03 ± 0.04^{d}	19.56 ± 0.64^{c}	56.96 ± 1.37^{bc}
T13		2:1	18.33 ± 0.32^{c}	61.01 ± 0.59^{c}	13.67 ± 0.70^{e}	67.42 ± 3.51^{ab}
T14		5:1	20.19 ± 1.23^{bcd}	57.05 ± 2.52^{cd}	17.37 ± 1.65^{cde}	60.87 ± 4.28^{abc}
T15	*T. harzianum* + *B. amyloliquefaciens* + Y9	1:1:1	14.80 ± 0.45^{f}	68.23 ± 1.29^{a}	15.24 ± 1.03^{de}	67.66 ± 2.85^{a}
T16		4:1:1	15.93 ± 0.74^{ef}	66.10 ± 1.37^{ab}	15.64 ± 0.42^{de}	66.27 ± 0.54^{a}
T17	*T. atroviride* + *B. amyloliquefaciens* + Y9	1:1:1	18.18 ± 0.54^{cd}	61.05 ± 1.45^{bc}	17.18 ± 0.66^{cd}	62.74 ± 1.10^{a}
T18		4:1:1	20.21 ± 1.78^{bcde}	57.00 ± 3.71^{cd}	17.54 ± 0.74^{cd}	60.51 ± 2.12^{abc}
T19	*T. harzianum* + *T. atroviride* + *B. amyloliquefaciens* + Y9	1:1:1:1	16.39 ± 0.33^{de}	65.13 ± 0.03^{ab}	17.17 ± 0.88^{cd}	63.77 ± 1.63^{a}
T20		2:2:1:1	15.92 ± 0.49^{ef}	66.13 ± 0.88^{a}	15.25 ± 1.12^{de}	66.91 ± 2.49^{a}

Trichoderma spp. inocula (10^6 conidia mL^{-1}) were pre-cultured for 48 h, subsequently the corresponding amount of *Bacillus* spp. inocula ($OD_{600} = 0.5$, approximately 6×10^6 CFU mL^{-1}) was inoculated into the preculture medium and incubated for another 48 h. For pure culture, *Trichoderma* spp. or *Bacillus* spp. was singly inoculated and incubated in shaker for 4 days. Data were mean ± SEM. Different letters mean significantly different according to Welch ANOVA ($P < 0.05$)

30 °C for 3 days. The colony diameters were determined by applying the 'crossing method' and photographed. The antifungal activity was then evaluated by measuring the fungal growth in the presence and absence of biocontrol agents. The experiment was repeated twice with three replications.

$$\text{Inhibition } (\%) = (\text{control growth} - \text{fungal growth}) / \text{control growth} \times 100\%$$

Biocontrol assays under controlled conditions

Healthy and consistent two-year-old coptis plants were transplanted at a rate of two plants per pot (12 × 12 × 10.5 cm), and each treatment contained three pots. The spore suspension of *F. solani* (5×10^6 conidia·mL^{-1}, 15 mL) was added to the pot. After 7 days, the suspension of Y9 isolate ($OD_{600} = 1.0$, 15 mL) was added to the pot of biocontrol group, and then 15 mL of Y9 isolate suspension was added every 10 d for a total of three times. Meanwhile, an equal volume of sterile water was added to the other groups. There were four treatments in this experiment, namely pathogenic fungi (*F. solani*, Fs), biocontrol (Fs + Y9), control (Y9) and sterile water (negative control). All the treated coptis plants were grown at 24 °C in the greenhouse with weak natural light. After 30 days post inoculation, the plants were rated for root rot severity using a grading system for *Panax notoginseng* root rot disease with some modifications: 0, healthy; 1, roots were slightly discolored, and discolored roots were less than 10%; 2, roots turned brown, and brown roots were 10–40%, with no rot of fibrous roots; 3, roots turned brown, and discolored roots were 40–50%, with rot of fibrous roots; 4, roots turned dark brown, and discolored roots were 50–70%, with rot of fibrous roots; 5, roots turned black, and discolored roots were more than 70%, with rot of fibrous roots (Li et al. 2020).

$$\text{Disease index} = [\sum(\text{number of diseased plants at each level} \times \text{representative value at each level})] / (\text{number of total plants investigated} \times \text{highest representative value}) \times 100$$

Field trials

A field experiment was conducted in a plot of land with naturally occurring root rot disease at Fengmu village (108°29′28″E and 30°13′36″N), Shizhu county, Chongqing, China, with an average altitude of 1545 m. Irrigation root of three co-cultured combinations and four single isolates were conducted every three weeks for a total of three times. Additionally, a commercial formulation of *Trichoderma harzianum* T22 (WP, BioWorks) was used as a control. The experiment was set up as a completely randomized block design, consisting of nine treatments (Table 4) and three replicates, with a total of 27 plots (5 m^2 each). For each plot, 10 L of the 10-fold dilution of the fermentation products or 30 g of *T. harzianum* (WP) were applied, and equivalent water served as a control. The coptis plants were investigated and classified according to the grading system for *P. notoginseng* root rot disease in July, when was the peak incidence.

To determine whether there was or not a synergistic interaction in bacterial combinations, Colby's formula as described (Colby 1967) was used:

$$E1 = (X1 \times Y1 \times Z1)/\ 100^{(n-1)}.$$

$$E1 = 100 - E$$

$$X1 = 100 - X$$

$$Y1 = 100 - Y$$

$$Z1 = 100 - Z$$

Where E is the expected percent inhibition value of the combined biocontrol agents, X, Y and Z are the percent inhibition of corresponding biocontrol agents applied alone, and n is the number of biocontrol agents in the combination. A synergism is determined to be present when the combination produces a value higher than E and when the value is lower there is antagonism in the combination.

Table 4 Field efficacy evaluation of the combinations against coptis root rot

Treatment	Acronym	Control efficacy (%)	Expected value (%)
Water			
T. harzianum T22 (WP)	HC(WP)	27.06 ± 0.44 d	
T. harzianum	HC	27.26 ± 0.20 d	
T. atroviride	SL	25.06 ± 0.23 e	
B. cereus Y9	Y9	20.28 ± 0.27 f	
B. amyloliquefaciens	JDF	19.26 ± 0.25 f	
T. harzianum + Y9	HY	29.42 ± 0.22 c	42.01
T. harzianum + *B. amyloliquefaciens* + Y9	HYJ	63.85 ± 0.23 a	53.18
T. harzianum + *T. atroviride* + *B. amyloliquefaciens* + Y9	HLYJ	60.98 ± 0.05 b	64.91

HY: the co-culture of *Trichoderma harzianum* and Y9 (1:1, v/v); HYJ: the co-culture of *T. harzianum*, *Bacillus amyloliquefaciens* and Y9 (1:1:1, v/v); HLYJ: the co-culture of *T. harzianum*, *T. atroviride*, *B. amyloliquefaciens* and Y9 (2:2:1:1, v/v). Control efficacy was measured by the reduction in disease index as compared to the water control, and data were mean ± SEM. Different letters mean significantly difference at $P < 0.05$ (Duncan test). Expected value was calculated based upon Colby's formula for synergism in any combinations

Statistical analysis

Unless otherwise indicated, all measurements were carried out in triplicate and were repeated at least twice, with reproducible results. Independent-samples *t* test was used to estimate the differences of disease index between "Fs" and "Fs + Y9". Welch ANOVA with Games-Howell post-hoc test was performed to analyze the mycelial growth, inhibition rate and disease index using the SPSS 22.0. All values were given as mean ± SEM, and different letters indicated significant differences at $P < 0.05$.

Results

Identification of the Y9 isolate

Isolate Y9 formed pink colored colonies with white precipitation ring on mannitol-egg-yolk-polymyxin agar (MYP), indicating that Y9 was mannitol negative and lecithinase positive (Fig. 1a). On NA plates, the colonies of isolate Y9 were white, opaque, extended edges, and surface rough as frosted glass or dissolved wax (Fig. 1b). Through the observation of gram staining and spore staining, the Y9 was a Gram-positive, rod-shaped, and spore producing bacterium (Fig. 1c, d). Parasporal crystals were observed in *B. thuringiensis* (Fig. 1e), but not in Y9 (Fig. 1f). Morphological characters indicated that isolate Y9 likely belonged to the genus *Bacillus*.

Blast results of the 16S rRNA sequence (OP897300) of isolate Y9 showed that isolate Y9 was most closely related to *Bacillus cereus* (100%) and *Bacillus thuringiensis* (100%). Similarly, the *gyrA* (OP909708) sequences of isolate Y9 were 100% identical to *B. thuringiensis* and *B. cereus*, and *rpoB* (OP909710) had 99.87% identity to *B. thuringiensis* and *B. cereus*. None of the three genes used alone were able to distinguish isolate Y9 from *B. thuringiensis* and *B. cereus*. Then a multilocus phylogeny of isolate Y9 and its relatives based on the three house-keeping genes (Fig. 2) was reconstructed using PhyloSuite, which indicated that Y9 isolate was clustered with *Bacillus cereus*.

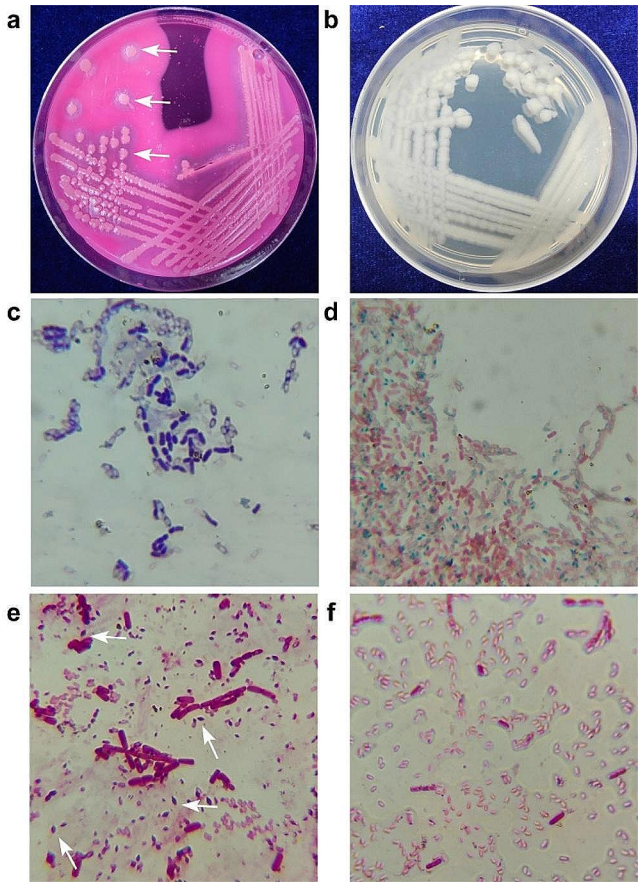

Fig. 1 The morphological characteristics of *Bacillus cereus* isolate Y9. Colonies of isolate Y9 grown on MYP (**a**) and NA (**b**) after 24 h of incubation at 30°C. **c** Gram staining and **d** spore staining. Protein toxin crystallization test of *B. thuringiensis* (**e**) and Y9 (**f**) after 4 d of incubation at 30°C. The white arrow marks the precipitation ring and parasporal crystals

Physiological and biochemical characterics (Table 2) also revealed that isolate Y9 was identical with *B. cereus*, which could not produce the parasporal crystals. Based on the morphological, physiological and biochemical characteristics, and molecular genetic analysis, isolate Y9 was identified as *B. cereus*, and was preserved in China General Microbiological Culture Collection Center (CGMCC No. 26960), Beijing, China.

Antifungal activity of *B. cereus* isolate Y9

Antagonistic activity assays showed that *B. cereus* isolate Y9 inhibited the growth of *F. solani* and *F. avenaceum*, which were the pathogens causing root rot of *C. chinensis*. The results showed that *B. cereus* isolate Y9 significantly inhibited the growth of *F. solani* and *F. avenaceum*, with a reduction in mycelial growth by 51.60% and 54.03%, respectively. The inhibitory effect of *B. cereus* isolate Y9 was similar to that of *B. amyloliquefaciens*, and better than that of *B. subtilis* (Fig. 3). The growth of seven other pathogens (*F. oxysporum*, *F. graminearum*, *F. fujikuroi*, *Clonostachys rosea*, *Collteotrichum fructicola*, *Collteotrichum gloeosporiodies*, and *Pestalotiopsis olivacea*) was also inhibited by *B. cereus* isolate Y9 (Fig. 4). The strongest inhibitory effect was against *F. graminearum* (44.20%), and the inhibition rate against *C. fructicola* and *C. gloeosporiodies* was about 40%. Overall, *B. cereus* isolate Y9 had a broad spectrum of antimicrobial activity, indicating a great potential in biocontrol.

Efficacy of *B. cereus* isolate Y9 against coptis root rot disease under controlled conditions

The ability of *B. cereus* isolate Y9 to inhibit *F. solani* in coptis plants was evaluated under greenhouse conditions. Disease severity was recorded 30 days post-inoculation by observing root discoloration. The coptis plants treated with *B. cereus* isolate Y9 only showed no symptoms in the root, and grew better than the mock treated plants. Typical symptoms and the highest disease severity can be observed in the control treatment which was inoculated with *F. solani* only. The coptis plants treated with *B. cereus* isolate Y9 in the presence of *F. solani* showed healthy with fewer symptoms in root compared with the control treatment, and the disease index was significantly reduced (Fig. 5). *B. cereus* isolate Y9 could effectively control root rot and significantly reduce the disease severity caused by *F. solani* on coptis plants.

Compatibility test

To determine the compatibility between Y9 and other biocontrol agents, in vitro assays were performed as previously described (Barbosa et al. 2018). Incompatible isolates showed inhibition halos regardless of the direction they were spread on the plates. In this study, a total of five isolates, including two isolates of *Bacillus* (*B. cereus*, Y9; *B. amyloliquefaciens*, JDF) and three isolates of *Trichoderma* (*T. harzianum*, HC; *T. atroviride*, SL; *T. reesei*, LS) were tested for the compatibility in all possible combinations of two isolates. Only isolate LS was inhibited by the two *Bacillus* bacteria, while the other eight combinations were compatible (Fig. 6). The same responses were observed on PDA and NA media and in another independent experiment. Only compatible combinations were tested in further experiments.

Antifungal activity of the combinations in vitro

The *B. cereus* isolate Y9 (T1) had a similar inhibitory effect on the growth of pathogenic fungi with *B. amyloliquefaciens*

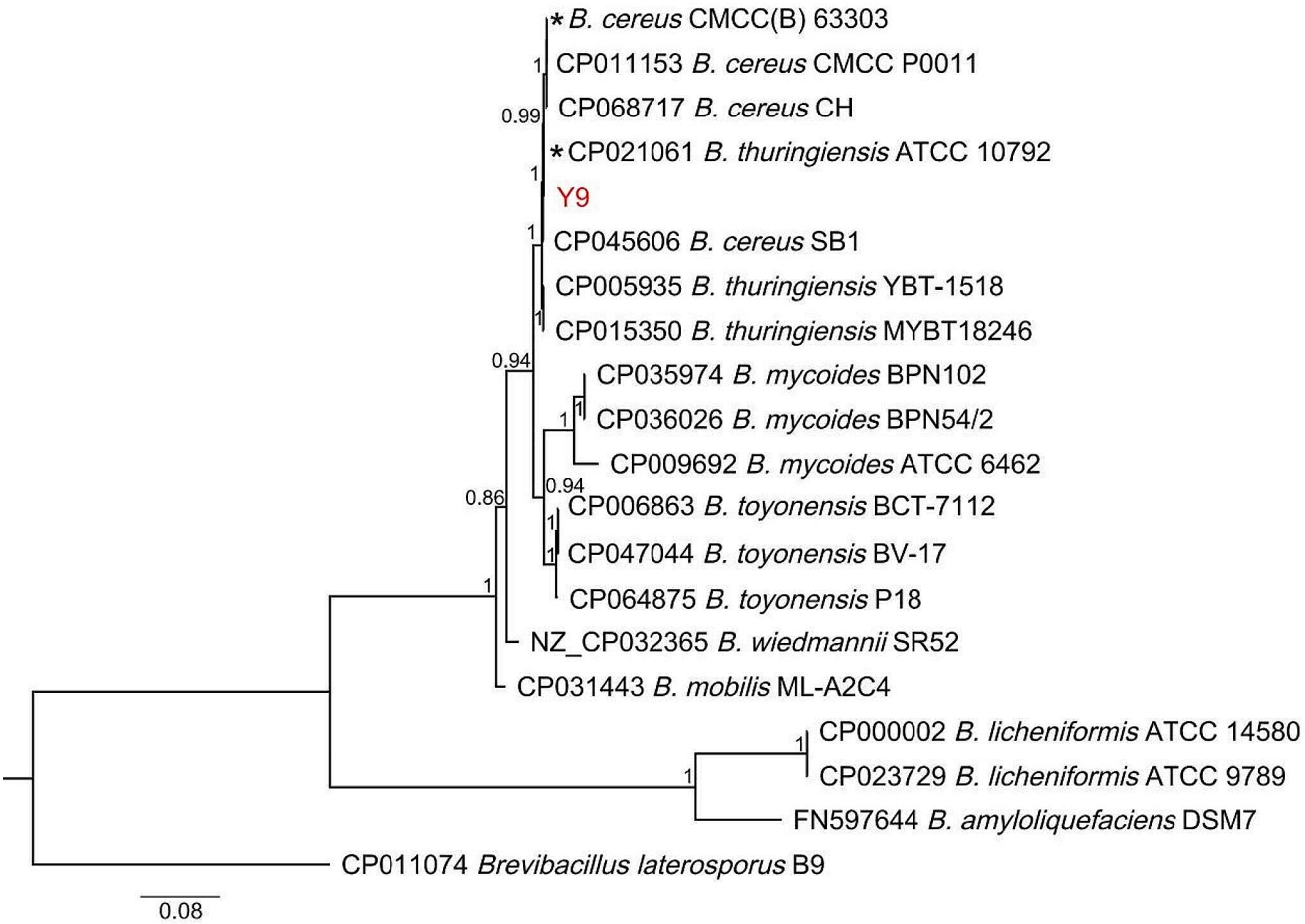

Fig. 2 Phylogenetic reconstruction of the isolate Y9 and its close relatives based on concatenated 16S rRNA, *gyrA* and *rpoB* nucleotide sequences. Phylogenetic analysis was conducted under Bayesian Inference (BI) criteria, and values above branches indicate BI posterior probabilities (pp). The bar indicates sequence divergence. The isolate Y9 was highlighted in red, and *B. cereus* (CMCC(B) 63303) and *B. thuringiensis* (ATCC 10792) were highlighted with an asterisk

(T2), but lower than *T. harzianum* (T3) or *T. atroviride* (T4), while the antifungal activities increased when *T. harzianum* or *T. atroviride* was mixed in co-culture (Table 3). All the treatments were effective in reducing the mycelial growth of the pathogens. However, the top five effective combinations against *F. solani* were T15 (68.23 ± 1.29), T9 (66.68 ± 0.08), T7 (66.58 ± 0.05), T5 (66.18 ± 0.22), T20 (66.13 ± 0.88), and T7 (68.52 ± 2.52), T15 (67.66 ± 2.85), T13 (67.42 ± 3.51), T6 (67.04 ± 2.11), T20 (66.91 ± 2.49) against *F. avenaceum* (Table 2). Combinations T7 (HY, *T. harzianum* + Y9, in ratio of 1:1), T15 (HYJ, *T. harzianum* + *B. amyloliquefaciens* + Y9, in ratio of 1:1:1) and T20 (HLYJ, *T. harzianum* + *T. atroviride* + *B. amyloliquefaciens* + Y9, in ratio of 2:2:1:1) had high inhibitory effect against both *F. solani* and *F. avenaceum*, and were selected for further field experiment.

Antagonistic efficacy of the combinations in the field

The field efficacy assessments showed that all the treatments reduced the disease index of coptis root rot, with a range from 19.26 to 63.85% (Table 4). The control efficacy of *Bacillus* isolates Y9 and JDF showed no significant difference, but was significantly lower than that of *Trichoderma* isolates HC and SL. The optimum combinations exhibited significantly higher antagonistic efficacy when compared to individual isolates. HYJ showed the highest control efficacy of 63.85%, which was higher than the expected value (53.18%), indicating synergistic effects on the control of coptis root rot. Interestingly, synergistic effect was only found in HYJ, but not HY or HLYJ. The results indicated the combinations of *B. cereus* isolate Y9 and *Trichoderma* spp. can be used as BCAs to control coptis root rot disease, and provided significantly better control efficacy than single *T. harzianum* (WP).

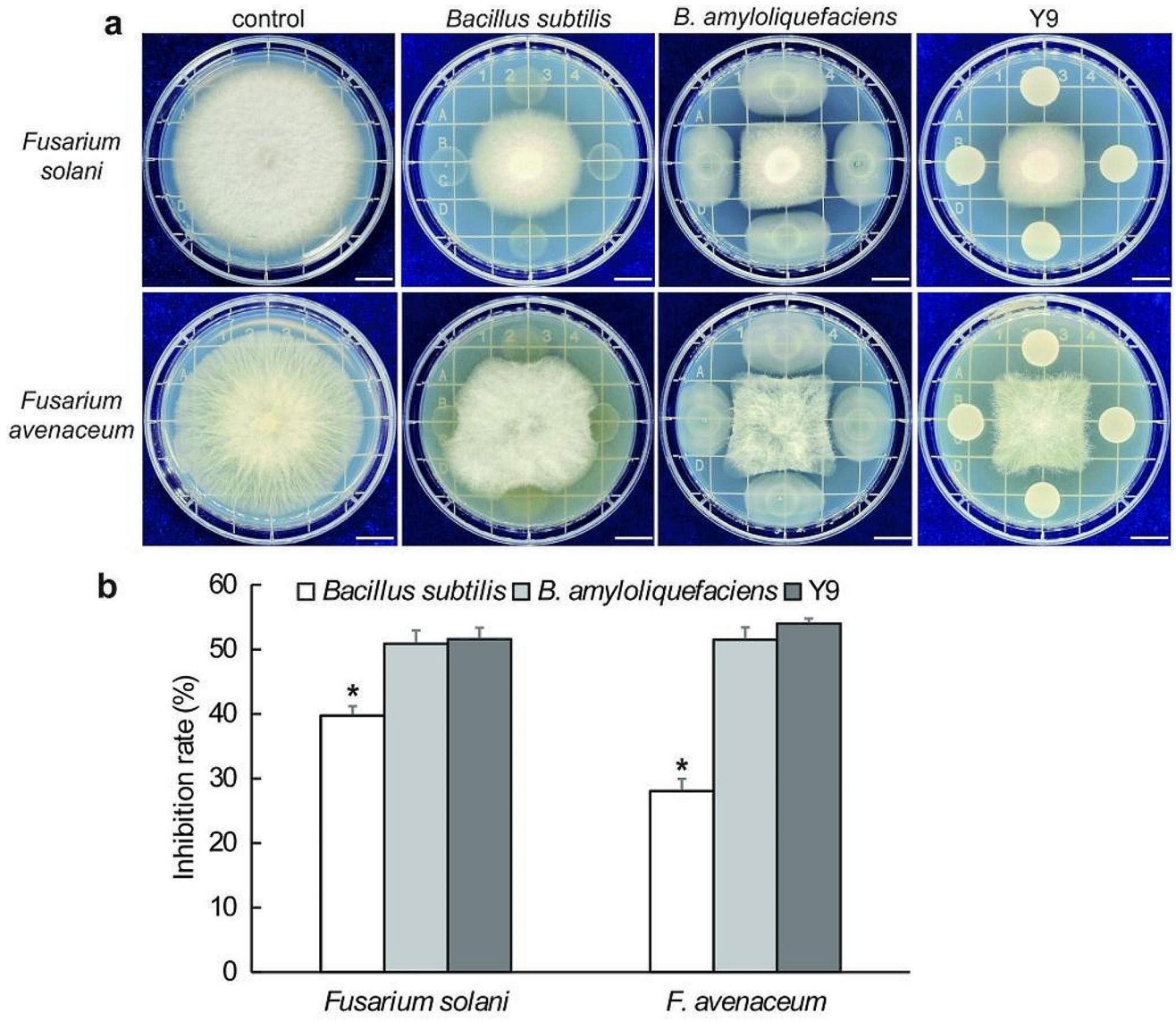

Fig. 3 Antagonistic activity of *Bacillus cereus* isolate Y9 against *Fusarium solani* and *F. avenaceum* in vitro. **a** Fungi treated with *B. subtilis* (ATCC 6633), *B. amyloliquefaciens* (CGMCC 1.15674) and *B. cereus* isolate Y9. Scale bars, 1 cm; **b** Inhibition rate of the *Bacillus* strains against *F. solani* and *F. avenaceum*. Values are means of three replicates for each treatment and bars indicate SEs. Asterisk indicates statistically significant ($P < 0.05$)

Discussion

In this study, isolate Y9 was isolated from the healthy fibrous roots of coptis plants, and showed strong antifungal activity against *F. solani* and *F. avenaceum*, with the inhibition rate of 51.60% and 54.03%, respectively. By comparing 16S rRNA gene sequences, we found that the isolate Y9 belonged to the genus *Bacillus*. But 16S rRNA sequences are not sufficient to discriminate *Bacillus* species and related genera, which share very similar 16S rRNA gene sequences (Xu and Cote 2003; Ehling-Schulz et al. 2019).Housekeeping genes *gyrA* and *rpoB* were reported to provide better phylogenetic resolution than 16S rRNA, and can be used to identify *Bacillus* species (Ki et al. 2009; Masum et al. 2018; Liu et al. 2022). However, we could not determine whether isolate Y9 was *B. thuringiensis* or *B. cereus*, no matter which marker genes were used alone. It is difficult to separate the *B. cereus* group (e.g. *B. cereus* and *B. thuringiensis*) by using molecular comparisons. Although the *rpoB* gene could be used to identify some members of the *B. cereus* group, but failed to discriminate between *B. thuringiensis* and *B. cereus* (Ki et al. 2009). Then, we present a multilocus phylogeny of the

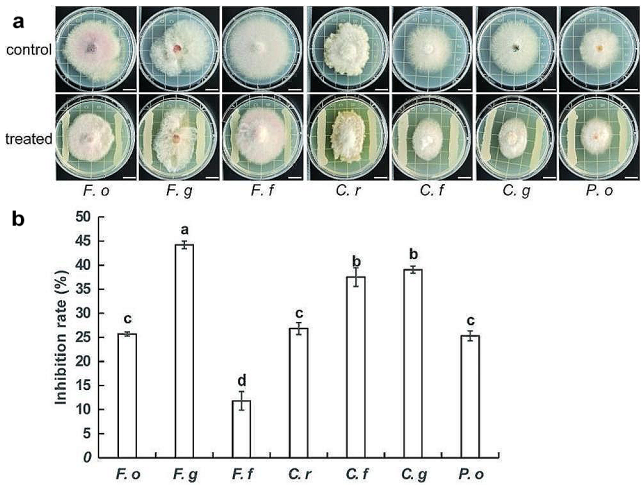

Fig. 4 Antagonistic activity of *Bacillus cereus* isolate Y9 against seven other pathogens in vitro. **a** Top row, untreated fungi used as the control; second row, fungi treated with *B. cereus* isolate Y9. Scale bars, 1 cm; **b** the inhibition rate of *B. cereus* isolate Y9 against seven other pathogens. F.o: *Fusarium oxysporum*, F.g: *F. graminearum*, F.f: *F. fujikuroi*, C.r: *Clonostachys rosea*, C.f: *Colletotrichum fructicola*, C.g: *Colletotrichum gloeosporiodies*, P.o: *Pestalotiopsis olivacea*. Values are means of three replicates for each treatment and bars indicate SEs. Columns with different letters indicate significant difference ($P < 0.05$)

isolate Y9 and its relatives based on all of the three molecular markers (16S rRNA, *gyrA* and *rpoB*), and found that isolate Y9 was clustered with *B. cereus* (Fig. 2). To provide more reliable results, we also conducted the protein toxin crystallization test on isolate Y9, with *B. cereus* (CMCC(B) 63303) and *B. thuringiensis* (ATCC 10792) as controls. The results showed that isolate Y9 was identical with *B. cereus*, which could not form the parasporal crystals.

Although some *B. cereus* isolates are commonly referred to food poisoning agents (Ehling-Schulz et al. 2019), several strains of *B. cereus* exhibit plant growth-promoting traits and show biocontrol capabilities against various plant pathogens (Kulkova et al. 2023). For example, seed bacterization of maize with *B. cereus sensu lato* strain B25 not only significantly reduced *Fusarium* stalk rot and *Fusarium* ear rot incidence and severity, but also significantly increased grain yield and reduced Fumonisin contamination up to 93.9% (Lizárraga-Sánchez et al. 2015). In this work, the antagonistic traits of *B. cereus* isolate Y9 against *F. solani* and *F. avenaceum* were evaluated (Fig. 3). Antagonism assay on PDA plates revealed the antimicrobial activity of *B. cereus* isolate Y9 against *F. solani* and *F. avenaceum*, with inhibition rates of 51.60% and 54.03%, respectively. The results showed that *B. cereus* isolate Y9 seemed to be less efficient than *T. harzianum* and *T. atroviride* (Table 3). Differences in growth rate might be a factor for relative low antifungal activity of Y9, since the growth rate of *Trichoderma* spp. on PDA is about 30 mm/d (Tian et al. 2023), while *Bacillus* spp. grows along the inoculation line (or site) and spreads slowly on PDA (Izquierdo-García et al. 2020). Notably, the antagonistic efficiency of *B. cereus* isolate Y9 was significantly higher than that of *B. subtilis*, a well known antagonistic bacterium. Similar results were found by Kushwaha et al. (2020) with *B. cereus* EPP5 the highest inhibitor for *F. solani*, followed by *B. amyloliquefaciens* EPP62 and *B.subtilis* EPP65. Moreover, the growth of other pathogens was also significantly inhibited (Fig. 4), indicating that *B. cereus* isolate Y9 exhibited a significant inhibitory effect on plant pathogens. According to Tian (2017), the sterile culture filtrate of *B. cereus* TJB-8 effectively inhibited the hyphae growth of *F. oxysporum*, *F. graminearum* and *C. gloeosporioides*, which is compatible with the current study. In the present study, *B. cereus* isolate Y9 displayed a protective effect against coptis root rot under greenhouse conditions (Fig. 5). However, the protective effect of *B. cereus* isolate Y9 was less effective compared to results reported by Kushwaha et al. (2020) where *B. cereus* EPP5 protected the pearl millet plants against *F. solani* under greenhouse conditions by 45.74%. Many factors influenced the control efficiency, including temperature, host plants, the specific strains and population density of BCAs. For example, the population density of *B. cereus* B8W8 was relatively higher in citrus than in apple at the same condition (Khadiri et al. 2023).

One of the important biocontrol mechanisms against phytopathogens present in *Bacillus* spp. is the production of antimicrobial substances. *B. cereus* genomes show a high abundance of cyclic lipopeptides gene clusters (e.g., iturin A, C, D; fengycin D; and surfactin A, C) (Kulkova et al. 2023). It was repotred that *B. cereus* XZ30-2 culture filtrate could produce hydrolases and lipopeptides (including iturin, surfactin and fengycin) and led to the intracellular leakage and nucleic acids release, and reactive oxygen species (ROS) accumulation in *Aspergillus niger* (Yi et al. 2023). Moreover, fengcin was found to play a vital role in inhibiting growth of *F. graminearum*, by damaging the plasma membranes and cell walls, and also inhibiting DNA synthesis of *F. graminearum* (Hanif et al. 2019). The activity of lytic enzymes (e.g. glucanases, proteases, cellulases, chitinases and chitosanases), which efficiently hydrolyze the main components of fungal cell walls, is another biocontrol mechanism of fungi in *Bacillus* spp. (Kulkova et al. 2023). For instance, 10% cell free supernatant of *B. amyloliquefaciens* FX2 damaged the cell ultrastructure, resulting in a remarkable increase in cellular leakage in *Botryosphaeria dothidea* mycelia, and the antifungal constituents were composed mainly of antifungal proteins, such as serine protease, metallopeptidase, hydrolase, and flagellin (Li et al. 2022). To date, many volatile organic compounds (VOCs) with antifungal effects produced by *B. cereus* have been identified. For instance, the VOCs of *B. cereus* strain B8W8 have

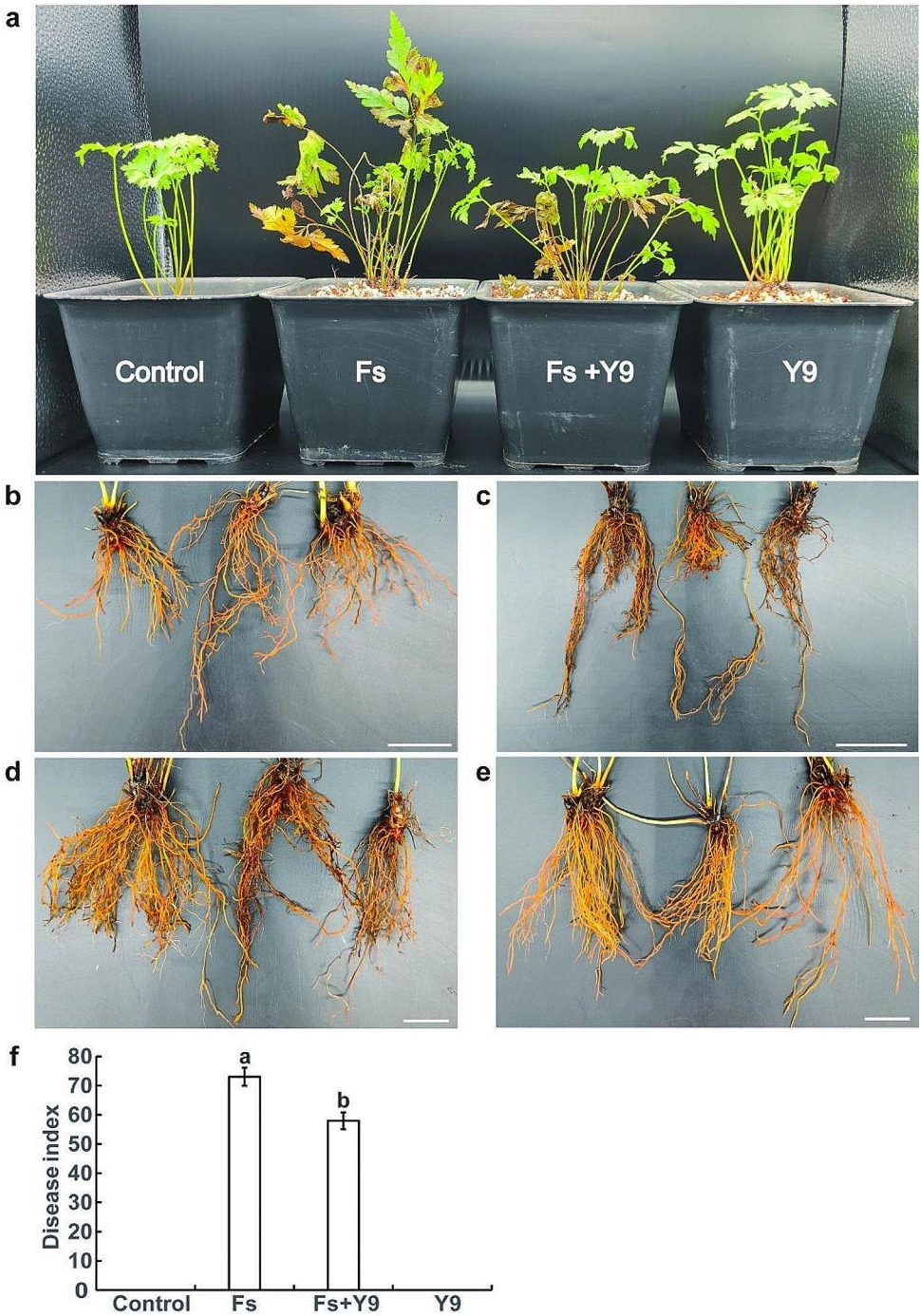

Fig. 5 Biocontrol of *Bacillus cereus* isolate Y9 against coptis root rot under controlled conditions. **a** Representative photographs of the coptis plants grown in pots in four different groups including Control (distilled water), Fs (*Fusarium solani*), Fs + Y9 (*F. solani* and *B. cereus*) and Y9 (*B. cereus*). The infected roots to show the root rot incidence of **b** Control, **c** Fs, **d** Fs + Y9, **e** Y9; **f** disease index of *F. solani* in mock and treated. Pictures were taken 30 days post inoculation. Values are means of three replicates for each treatment and bars indicate SEs. Columns with different letters indicate significant difference ($P < 0.05$). Scale bars, 2 m

high efficacy to inhibit the growth of *Monilinia laxa* and *M. fructigena* (Khadiri et al. 2023). The VOCs in *B. cereus* MH778713 promoted tomato seedling growth and showed antifungal activity against *F. oxysporum* (Ramírez et al. 2022). And five major VOCs released by *B. cereus* CF4-51 damaged the *Sclerotinia sclerotiorum* hyphae and inhibited the formation of sclerotia (Hu et al. 2023). In *B. cereus* B25, the chitinase and chitosanase activities were induced to inhibit the growth of the phytopathogen *F. verticillioides* P03 (Báez-Astorga et al. 2022).Another biocontrol mechanism of fungi present in *B. cereus* strains is by triggering induced systemic resistance (ISR), which requires salicylic acid (SA), jasmonic acid (JA), and ethylene (ET) signaling pathways (Nie et al. 2017). For example, *B. cereus* AR156 triggered ISR against *Pseudomonas syringae* pv. *tomato* DC3000 in *Arabidopsis* by simultaneously activating the SA- and JA/ET-signaling pathways in an NPR1 dependent manner (Niu et al. 2011). AR156 were able to increase the

a

	Isolates				
	Y9	JDF	HC	SL	LS
Y9		+	+	+	-
JDF	+		+	+	-
HC	+	+		+	+
SL	+	+	+		+
LS	-	-	+	+	

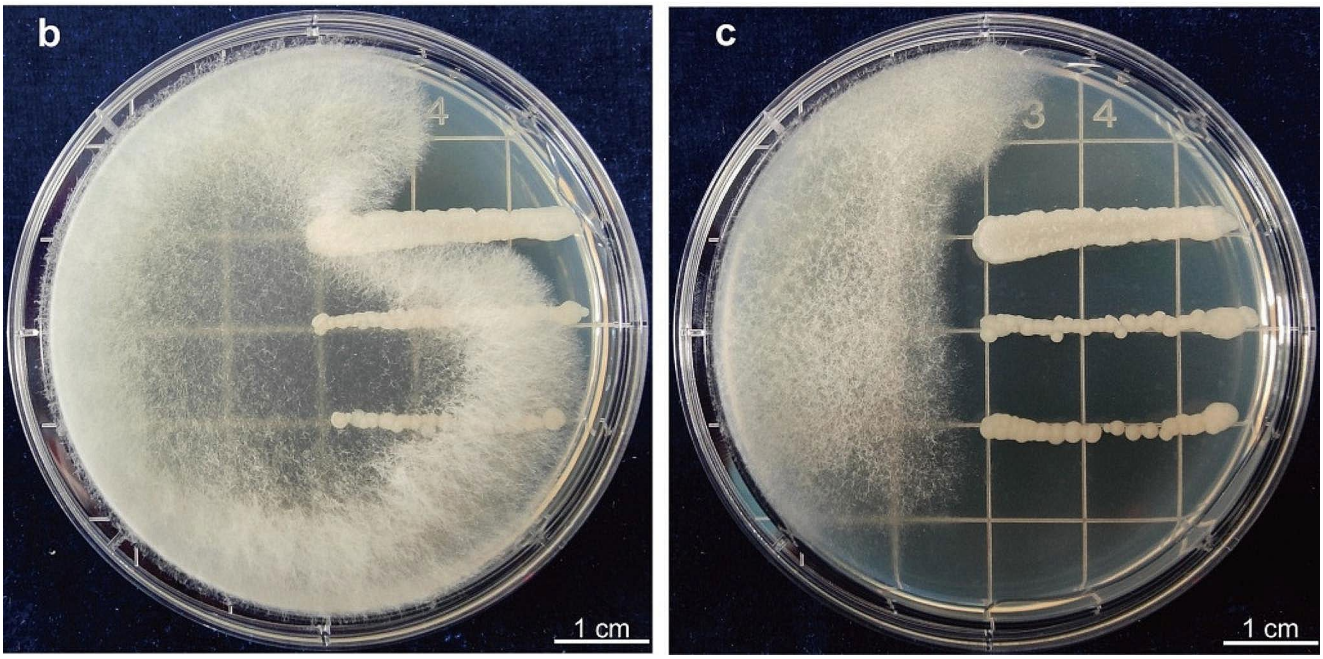

Fig. 6 Compatibility between biocontrol agents on agar plates. **a** The plus signal indicates a compatible combination and a minus indicates an incompatible combination; **b** Compatible and **c** incompatible combinations on plates. Y9, *Bacillus cereus*; JDF, *B. amyloliquefaciens*; HC, *Trichoderma harzianum*; SL, *T. atroviride*; LS, *T. reesei*. Scale bars, 1 cm

average biomass of the tomato by 47.7%, and decrease bacterial speck disease severity by 1.6-fold, via simultaneous activation of the SA- and JA-signaling pathways (Niu et al. 2012). However, JA/ET-signaling pathways and NPR1, but not SA-, were activated by AR156-induced ISR against *B. cinerea* in *Arabidopsis* (Nie et al. 2017). Therefore, we hypothesized that the main biocontrol mechanism of *B. cereus* isolate Y9 is also antibiotics and ISR in plants (Fig. 7).

Combined use of BCAs is more effective than using a single strain (Poveda and Eugui 2022). Almost all the combinations tested improved the inhibition rate in dual culture assay (Table 3). However, only in 10 of the total 465 published treatments was there evidence for synergistic effects among BCAs (Xu et al. 2011a). In most cases, combined use of two BCAs with different biocontrol mechanisms only achieved biocontrol efficacies similar to those achieved by the more efficacious one alone (Xu et al. 2011b). It seemed that antagonistic interactions were more likely to occur among BCAs than synergistic interactions. However, it is worth noting that, plant defense can be more effective when combined application of several biocontrol agents are used, compared with the application of a single biocontrol strain, although no statistical analysis is done to prove the existence of synergism numerically. When the inoculation proportion between *B. amyloliquefaciens* ACCC11060 and *T. asperellum* GDFS1009 was 1.9:1, it could produce more specific antimicrobial substances than single inoculation, and exhibited the highest antifungal effect on *B. cinerea* (66.86%) (Wu et al. 2018). Similarly, co-cultivation of *T. asperellum* GDFS1009 and *B. amyloliquefaciens* 1841 significantly enhanced biocontrol activity against *F.*

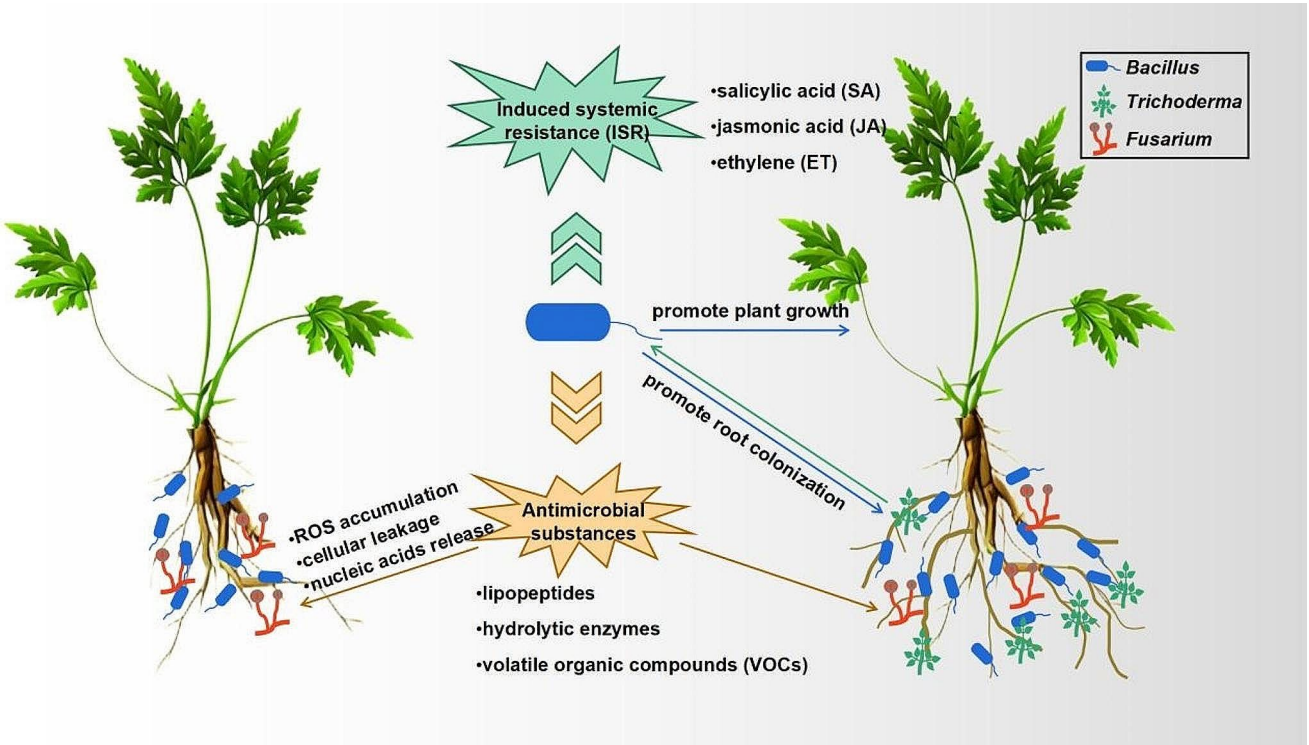

Fig. 7 Antifungal mechanisms of *Bacillus* and *Trichoderma* alone or in combination

graminearum, *F. oxysporum* and *B. cinerea*, and improved the wheat growth (Karuppiah et al. 2019a). Single treatment of *B. cereus* (EPP5), *B. amyloliquefaciens* (EPP62) or *B. subtilis* (EPP65) offered protection ranging from 35.68 to 45.74% under greenhouse conditions. However, the co-culture (EPP5 + EPP62 + EPP65) provided the highest protection (71.96%) against *F. solani* with significant increase in pearl millet (*Pennisetum glaucum*) biomass (Kushwaha et al. 2020). It was reported that *Bacillus* spp. and *Trichoderma* spp. act synergistically to enhance root colonization rate for each other. Root colonization of *T. harzianum* OMG16 increased up to 10-fold in the presence of *B. velezensis* FZB42, and the presence of OMG16 increased the root colonization rate of FZB42 significantly, too (Hafiz et al. 2022). In this study, more fine roots were induced by HYJ and HLYJ treatment (data not shown) demonstrated that *Bacillus* spp. and *Trichoderma* spp. were able to stimulate fine-root formation, which subsequently provides increased potential sites for plants and fungi to interact (Fig. 7).

In this study, Colby's formula was used to evaluate the expected synergism in combination of two to four BCAs. Colby's formula was developed from Limpel's formula (Richer 1987), which was widely used in studies of synergy with fungicide mixtures and biocontrol of plant diseases (Barbosa et al. 2018; Yaderets et al. 2021; Öztekin and Karbancioglu-Guler 2023). Thus, we think Colby's formula seems equally applicable for fungicides. Our results showed that only the combination of HYJ, but not HLYJ, exhibited synergistic effects on the control of coptis root rot. Antagonistic activity of the BCAs in HLYJ treatment might be affected by each other, but not in HYJ treatment. The inoculation ratio of HLYJ was 2:2:1:1, and the high concentration of antimicrobial compounds produced by *Trichoderma* spp. might negatively affected the growth and biocontrol activity of *Bacillus*. Since it was reported that exposing *B. velezensis* Bs006 to *T. virens* Gl006-supernatant negatively affected the growth of the bacteria, biofilm formation and biocontrol activity, in a concentration dependent manner, although its viability and antagonistic ability was not affected (Izquierdo-García et al. 2020). A synergistic effect, forming more stable rhizosphere communities and occupying different or complementary niches may be the antagonistic mechanisms of the co-culture of *Bacillus-Trichoderma* (Poveda and Eugui 2022). It was reported that BCAs with different mechanisms have a higher chance of acting synergistically, as compared to BCAs with the same mechanisms, and BCAs with both mycoparasitism and competition mechanisms was more effective over the range of parameter values evaluated (Xu et al. 2011b).

According to the investigation in the field, *Coptis* root rot generally started to occur from March to April, and the peak incidence was from May to July, then gradually decreased after September. Based on the occurrence of *Coptis* root rot, the *B. cereus* isolate Y9 and its combinations were first

applied in April for a total of three times, at three weeks intervals, and the incidence of the disease was investigated in July. The long-term effects of *B. cereus* isolate Y9 and its combinations on the coptis root rot need to be assessed in more seasons and locations, under different environmental conditions and disease pressure.

Conclusions

Isolate Y9 which was isolated from the healthy roots of coptis, was identified as *B. cereus* based on the morphological, physiological and biochemical characteristics, and molecular genetic analysis. The *B. cereus* isolate Y9 had inhibitory effects on *F. solani* and *F. avenaceum* and seven strains of other pathogenic fungi. In this study, combined use of *T. harzianum*, *B. amyloliquefaciens* and *B. cereus* isolate Y9 (HYJ, in ratio of 1:1:1) led to a synergistic effect in controlling coptis root rot in the field. The underlying mechanism and more field application deserve further investigation.

Funding This work was supported by the Technological Innovation and Application Development Project of Traditional Chinese Medicine (No. 2021ZY3814), Key Project for Technological Innovation and Application Development in Chongqing (cstc2021jscx-dxwtBX0014) and the earmarked fund for CARS-21.

Data availability The data that support the findings of this study are available from the corresponding author upon reasonable request.

Declarations

Ethical approval The authors declare that ethical standards have been followed and that no human participants or animals were involved in this research.

Competing interests The authors have no competing interests to declare that are relevant to the content of this article.

Open Access This article is licensed under a Creative Commons Attribution 4.0 International License, which permits use, sharing, adaptation, distribution and reproduction in any medium or format, as long as you give appropriate credit to the original author(s) and the source, provide a link to the Creative Commons licence, and indicate if changes were made. The images or other third party material in this article are included in the article's Creative Commons licence, unless indicated otherwise in a credit line to the material. If material is not included in the article's Creative Commons licence and your intended use is not permitted by statutory regulation or exceeds the permitted use, you will need to obtain permission directly from the copyright holder. To view a copy of this licence, visit http://creativecommons.org/licenses/by/4.0/.

References

Báez-Astorga PA, Cázares-Álvarez JE, Cruz-Mendívil A, Quiroz-Figueroa FR, Sánchez-Valle VI, Maldonado-Mendoza IE (2022) Molecular and biochemical characterisation of antagonistic mechanisms of the biocontrol agent *Bacillus cereus* B25 inhibiting the growth of the phytopathogen *Fusarium verticillioides* P03 during their direct interaction *in vitro*. Biocontrol Sci Technol 32:1074–1094. https://doi.org/10.1080/09583157.2022.2085662

Balthazar C, Novinscak A, Cantin G, Joly DL, Filion M (2022) Biocontrol activity of *Bacillus* spp. and *Pseudomonas* spp. against *Botrytis Cinerea* and other cannabis fungal pathogens. Phytopathology 112:549–560. https://doi.org/10.1094/phyto-03-21-0128-r

Barbosa LO, Lima JS, Magalhães VC, Gava CAT, Soares ACF, Marbach PAS, Souza JT (2018) Compatibility and combination of selected bacterial antagonists in the biocontrol of sisal bole rot disease. Biocontrol 63:595–605. https://doi.org/10.1007/s10526-018-9872-x

Behiry S, Soliman SA, Massoud MA, Abdelbary M, Kordy AM, Abdelkhalek A, Heflish A (2023) *Trichoderma pubescens* elicit induced systemic resistance in tomato challenged by *Rhizoctonia solani*. J Fungi 9:167. https://doi.org/10.3390/jof9020167

Capella-Gutiérrez S, Silla-Martínez JM, Gabaldón T (2009) trimAl: a tool for automated alignment trimming in large-scale phylogenetic analyses. Bioinformatics 25:1972–1973. https://doi.org/10.1093/bioinformatics/btp348

Cheng HH, Yang F, Gao J, Tan DM, Zhang MX, Ding HX (2020) Identification and fungicide sensitivity of pathogen causing root rot of goldthread. Acta Phytopathologica Sinica 50:377–380. https://doi.org/10.13926/j.cnki.apps.000329

Colby SR (1967) Calculating synergistic and antagonistic responses of herbicide combinations. Weeds 15:20–22. https://doi.org/10.2307/4041058

Coleman JJ, Rounsley SD, Rodriguez-Carres M, Kuo A, Wasmann CC, Grimwood J, Schmutz J, Taga M, White GJ, Zhou S, Schwartz DC, Freitag M, Ma LJ, Danchin EG, Henrissat B, Coutinho PM, Nelson DR, Straney D, Napoli CA, Barker BM, Gribskov M, Rep M, Kroken S, Molnár I, Rensing C, Kennell JC, Zamora J, Farman ML, Selker EU, Salamov A, Shapiro H, Pangilinan J, Lindquist E, Lamers C, Grigoriev IV, Geiser DM, Covert SF, Temporini E, Vanetten HD (2009) The genome of *Nectria Haematococca*: contribution of supernumerary chromosomes to gene expansion. PLoS Genet 5:e1000618. https://doi.org/10.1371/journal.pgen.1000618

Commission CP (2020) Pharmacopoeia of the people's republic of China, 2020 edn. vol. I. China Medical Science Press, Beijing, pp 177

Dong XZ, Cai MY (2001) Systemic identification manual of common bacteria. Science, Beijing, pp 353–384

Ehling-Schulz M, Lereclus D, Koehler TM (2019) The *Bacillus cereus* group: *Bacillus* species with pathogenic potential. Microbiol Spectr 7. https://doi.org/10.1128/microbiolspec.GPP3-0032-2018.:GPP3-0032-2018

Frank JA, Reich CI, Sharma S, Weisbaum JS, Wilson BA, Olsen GJ (2008) Critical evaluation of two primers commonly used for amplification of bacterial 16S rRNA genes. Appl Environ Microbiol 74:2461–2470. https://doi.org/10.1128/AEM.02272-07

Gao Z, Zhang B, Liu H, Han J, Zhang Y (2017) Identification of endophytic *Bacillus velezensis* ZSY-1 strain and antifungal activity of its volatile compounds against *Alternaria solani* and *Botrytis Cinerea*. Biol Control 105:27–39. https://doi.org/10.1016/j.biocontrol.2016.11.007

Hafiz FB, Moradtalab N, Goertz S, Rietz S, Dietel K, Rozhon W, Humbeck K, Geistlinger J, Neumann G, Schellenberg I (2022) Synergistic effects of a root-endophytic *Trichoderma* fungus and *Bacillus* on early root colonization and defense activation against *Verticillium Longisporum* in rapeseed. Mol Plant Microbe Interact 35:380–392. https://doi.org/10.1094/mpmi-11-21-0274-r

Han SY, Chen JX, Zhao YJ, Cai HS, Guo CH (2021) *Bacillus subtilis* HSY21 can reduce soybean root rot and inhibit the expression of genes related to the pathogenicity of *Fusarium oxysporum*. Pestic Biochem Physiol 178:104916. https://doi.org/10.1016/j.pestbp.2021.104916

Han PJ, Liu TR, Zheng Y, Song RQ, Nan TG, Yang XL, Huang LQ, Yuan Y (2022) A mycorrhizal bacteria strain isolated from *Polyporus umbellatus* exhibits broad-spectrum antifungal activity. Front Plant Sci 13:954160. https://doi.org/10.3389/fpls.2022.954160

Hanif A, Zhang F, Li PP, Li CC, Xu YJ, Zubair M, Zhang MX, Jia DD, Zhao XZ, Liang JG, Majid T, Yan JYA, Farzand A, Wu HJ, Gu Q, Gao XW (2019) Fengycin produced by *Bacillus amyloliquefaciens* FZB42 inhibits *Fusarium graminearum* growth and mycotoxins biosynthesis. Toxins 11:295. https://doi.org/10.3390/toxins11050295

Hasan N, Farzand A, Heng Z, Khan IU, Moosa A, Zubair M, Na Y, Ying S, Tang CM (2020) Antagonistic potential of novel endophytic *Bacillus* strains and mediation of plant defense against verticillium wilt in upland cotton. Plants-Basel 9:1438. https://doi.org/10.3390/plants9111438

Hashem AH, Abdelaziz AM, Askar AA, Fouda HM, Khalil AMA, Abd-Elsalam KA, Khaleil MM (2021) *Bacillus megaterium*-mediated synthesis of selenium nanoparticles and their antifungal activity against *Rhizoctonia solani* in faba bean plants. J Fungi 7:195. https://doi.org/10.3390/jof7030195

Hu JH, Dong BZ, Wang D, Meng HW, Li XJ, Zhou HY (2023) Genomic and metabolic features of *Bacillus cereus*, inhibiting the growth of *Sclerotinia sclerotiorum* by synthesizing secondary metabolites. Arch Microbiol 205:8. https://doi.org/10.1007/s00203-022-03351-5

Izquierdo-García LF, González-Almario A, Cotes AM, Moreno-Velandia CA (2020) *Trichoderma virens* Gl006 and *Bacillus velezensis* Bs006: a compatible interaction controlling Fusarium wilt of cape gooseberry. Sci Rep 10:6857. https://doi.org/10.1038/s41598-020-63689-y

Jiang CH, Liao MJ, Wang HK, Zheng MZ, Xu JJ, Guo JH (2018) *Bacillus velezensis*, a potential and efficient biocontrol agent in control of pepper gray mold caused by *Botrytis Cinerea*. Biol Control 126:147–157. https://doi.org/10.1016/j.biocontrol.2018.07.017

Kalyaanamoorthy S, Minh BQ, Wong TKF, Haeseler AV, Jermiin LS (2017) ModelFinder: fast model selection for accurate phylogenetic estimates. Nat Methods 14:587–589. https://doi.org/10.1038/NMETH.4285

Karuppiah V, Sun JN, Li TT, Vallikkannu M, Chen J (2019a) Co-cultivation of *Trichoderma Asperellum* GDFS1009 and *Bacillus amyloliquefaciens* 1841 causes differential gene expression and improvement in the wheat growth and biocontrol activity. Front Microbiol 10:16. https://doi.org/10.3389/fmicb.2019.01068

Karuppiah V, Vallikkannu M, Li T, Chen J (2019b) Simultaneous and sequential based co-fermentations of *Trichoderma Asperellum* GDFS1009 and *Bacillus amyloliquefaciens* 1841: a strategy to enhance the gene expression and metabolites to improve the biocontrol and plant growth promoting activity. Microb Cell Fact 18:185. https://doi.org/10.1186/s12934-019-1233-7

Katoh K, Standley DM (2013) MAFFT multiple sequence alignment software version 7: improvements in performance and usability. Mol Biol Evol 30:772–780. https://doi.org/10.1093/molbev/mst010

Khadiri M, Boubaker H, Askarne L, Ezrari S, Radouane N, Farhaoui A, El Hamss H, Tahiri A, Barka EA, Lahlali R (2023) *Bacillus cereus* B8W8 an effective bacterial antagonist against major postharvest fungal pathogens of fruit. Postharvest Biol Technol 200:112315. https://doi.org/10.1016/j.postharvbio.2023.112315

Ki JS, Zhang W, Qian PY (2009) Discovery of marine *Bacillus* species by *16S rRNA* and *rpoB* comparisons and their usefulness for species identification. J Microbiol Methods 77:48–57. https://doi.org/10.1016/j.mimet.2009.01.003

Kulkova I, Dobrzynski J, Kowalczyk P, Belzecki G, Kramkowski K (2023) Plant growth promotion using *Bacillus cereus*. Int J Mol Sci 24:9759. https://doi.org/10.3390/ijms24119759

Kushwaha P, Kashyap PL, Srivastava AK, Tiwari RK (2020) Plant growth promoting and antifungal activity in endophytic *Bacillus* strains from pearl millet (*Pennisetum glaucum*). Brazilian J Microbiol 51:229–241. https://doi.org/10.1007/s42770-019-00172-5

Li YB, Liu YX, Zhu SS, Luo LX, Li JQ (2020) Grading system for *Panax notoginseng* root rot disease. Acta Phytopathologica Sinica 50:450–461. https://doi.org/10.13926/j.cnki.apps.000468

Li Q, Hou ZQ, Zhou DQ, Jia MY, Lu SP, Yu JP (2022) Antifungal activity and possible mechanism of *Bacillus amyloliquefaciens* FX2 against the postharvest apple ring rot pathogen. Phytopathology 112:2486–2494. https://doi.org/10.1094/phyto-02-22-0047-r

Liu Y, Štefanič P, Miao Y, Xue Y, Xun W, Zhang N, Shen Q, Zhang R, Xu Z, Mandic-Mulec I (2022) Housekeeping gene *gyrA*, a potential molecular marker for *Bacillus* ecology study. AMB Express 12:133. https://doi.org/10.1186/s13568-022-01477-9

Lizárraga-Sánchez GJ, Leyva-Madrigal KY, Sánchez-Peña P, Quiroz-Figueroa FR, Maldonado-Mendoza IE (2015) *Bacillus cereus sensu lato* strain B25 controls maize stalk and ear rot in Sinaloa, Mexico. Field Crops Res 176:11–21. https://doi.org/10.1016/j.fcr.2015.02.015

Luo XM, Li JL, Dong JY, Sui AP, Sheng ML, Yang XY (2014) First report of *Fusarium solani* causing root rot on *Coptis chinensis* in southwestern China. Plant Dis 98:1273. https://doi.org/10.1094/pdis-02-14-0164-pdn

Ma QF, Cong YZ, Feng LT, Liu CY, Yang WH, Xin Y, Chen KS (2022) Effects of mixed culture fermentation of *Bacillus amyloliquefaciens* and *Trichoderma longibrachiatum* on its constituent strains and the biocontrol of tomato *fusarium wilt*. J Appl Microbiol 132:532–546. https://doi.org/10.1111/jam.15208

Masum MMI, Liu L, Yang M, Hossain MM, Siddiqa MM, Supty ME, Ogunyemi SO, Hossain A, An Q, Li B (2018) Halotolerant bacteria belonging to operational group *Bacillus amyloliquefaciens* in biocontrol of the rice brown stripe pathogen *Acidovorax oryzae*. J Appl Microbiol 125:1852–1867. https://doi.org/10.1111/jam.14088

Mazzola M, Freilich S (2017) Prospects for biological soilborne disease control: application of indigenous versus synthetic microbiomes. Phytopathology 107:256–263. https://doi.org/10.1094/phyto-09-16-0330-rvw

Mei PY, Song XH, Zhu ZY, Li LY (2021a) First report of *Diaporthe eres* causing root rot of *Coptis Chinensis* Franchet. Plant Dis 105:1854. https://doi.org/10.1094/PDIS-12-20-2564-PDN

Mei PY, Song XH, Zhu ZY, Li LY (2021b) First report of root rot caused by *Fusarium avenaceum* on *Coptis chinensis* in Chongqing, China. Plant Dis 105:496. https://doi.org/10.1094/PDIS-05-20-1110-PDN

Nie PP, Li X, Wang SN, Guo JH, Zhao HW, Niu DD (2017) Induced systemic resistance against *Botrytis cinerea* by *Bacillus cereus* AR156 through a JA/ET- and *NPR1*-dependent signaling pathway and activates PAMP-triggered immunity in *Arabidopsis*. Front Plant Sci 8:238. https://doi.org/10.3389/fpls.2017.00238

Niu DD, Liu HX, Jiang CH, Wang YP, Wang QY, Jin HL, Guo JH (2011) The plant growth-promoting rhizobacterium *Bacillus cereus* AR156 induces systemic resistance in *Arabidopsis thaliana* by simultaneously activating salicylate- and jasmonate/ethylene-dependent signaling pathways. Mol Plant Microbe Interact 24:533–542. https://doi.org/10.1094/MPMI-09-10-0213

Niu DD, Wang CJ, Guo YH, Jiang CH, Zhang WZ, Wang YP, Guo JH (2012) The plant growth-promoting rhizobacterium *Bacillus cereus* AR156 induces resistance in tomato with induction and

priming of defence response. Biocontrol Sci Technol 22:991–1004. https://doi.org/10.1080/09583157.2012.706595

Öztekin S, Karbancioglu-Guler F (2023) Biological control of green mould on mandarin fruit through the combined use of antagonistic yeasts. Biol Control 180:105186. https://doi.org/10.1016/j.biocontrol.2023.105186

Poveda J, Eugui D (2022) Combined use of *Trichoderma* and beneficial bacteria (mainly *Bacillus* and Pseudomonas): development of microbial synergistic bio-inoculants in sustainable agriculture. Biol Control 176:105100. https://doi.org/10.1016/j.biocontrol.2022.105100

Ramírez V, Martínez J, Bustillos-Cristales MD, Catañeda-Antonio D, Munive JA, Baez A (2022) *Bacillus cereus* MH778713 elicits tomato plant protection against *Fusarium oxysporum*. J Appl Microbiol 132:470–482. https://doi.org/10.1111/jam.15179

Ranwez V, Douzery EJP, Cambon C, Chantret N, Delsuc F (2018) MACSE v2: toolkit for the alignment of coding sequences accounting for frameshifts and stop codons. Mol Biol Evol 35:2582–2584. https://doi.org/10.1093/molbev/msy159

Richer DL (1987) Synergism—a patent view. Pest Sci 19:309–315. https://doi.org/10.1002/ps.2780190408

Ronquist F, Teslenko M, Mark PVD, Ayres DL, Darling A, Höhna S, Larget B, Liu L, Suchard MA, Huelsenbeck JP (2012) MrBayes 3.2: efficient bayesian phylogenetic inference and model choice across a large model space. Syst Biol 61:539–542. https://doi.org/10.1093/sysbio/sys029

Song XH, Mei PY, Dou T, Liu QD, Li LY (2023) Multi-omics analysis reveals the resistance mechanism and the pathogens causing root rot of *Coptis Chinensis*. Microbiol Spectr 11:e04803–04822. https://doi.org/10.1128/spectrum.04803-22

Tian A (2017) Antagonistic strain of TJB-8 and its antifungal substances. J Zhejiang Agric Forestry Univ 34:1071–1078. https://doi.org/10.11833/j.issn.2095-0756.2017.06.015

Tian M, Peng Y, Lu H, Qin N, Ren L, Yin H, Zhao X (2023) *Trichoderma Afroharzianum* LMNS-M9: identification, biological characteristics, and growth-promoting effect on quinoa. Microbiol China 50:3848–3865. https://doi.org/10.13344/j.microbiol.china.230144

Wei J, Zhao J, Suo M, Wu H, Zhao M, Yang H (2023) Biocontrol mechanisms of Bacillus velezensis against Fusarium oxysporum from Panax ginseng. Biol Control 182:105222. https://doi.org/10.1016/j.biocontrol.2023.105222

Wu Q, Ni M, Dou K, Tang J, Ren JH, Yu CJ, Chen J (2018) Co-culture of *Bacillus amyloliquefaciens* ACCC11060 and *Trichoderma asperellum* GDFS1009 enhanced pathogen-inhibition and amino acid yield. Microb Cell Fact 17:155. https://doi.org/10.1186/s12934-018-1004-x

Wu XL, Wang Y, Liu F, Chen DX, Li LY (2020) Identification of Coptis chinensis root rot disease pathogenic fusarium spp. fungi. China J Chin Materia Med 45:1323–1328. https://doi.org/10.19540/j.cnki.cjcmm.20200112.102

Wu X, Chen D, Liu F, Wang Y, Li L (2021a) Identification of *Coptis chinensis* root rot disease pathogenic fungi belonging to *Ilyonectria* spp. Southwest China J Agricultural Sci 34:299–305. https://doi.org/10.16213/j.cnki.scjas.2021.2.011

Wu X, Chen D, Liu F, Wang Y, Li L (2021b) Identification of the *Pythium* pathogen responsible for root rot of *Coptis Chinensis*. J Southwest Univ (Natural Sci Edition) 43:37–43. https://doi.org/10.13718/j.cnki.xdzk.2021.06.005

Xiang CY, Gao FL, Jakovlić I, Lei HP, Hu Y, Zhang H, Zou H, Wang GT, Zhang D (2023) Using PhyloSuite for molecular phylogeny and tree-based analyses. iMeta 2:e87. https://doi.org/10.1002/imt2.87

Xu D, Cote JC (2003) Phylogenetic relationships between *Bacillus* species and related genera inferred from comparison of 3' end 16S rDNA and 5' end 16S-23S ITS nucleotide sequences. Int J Syst Evol MicroBiol 53:695–704. https://doi.org/10.1099/ijs.0.02346-0

Xu XM, Jeffries P, Pautasso M, Jeger MJ (2011a) Combined use of biocontrol agents to manage plant diseases in theory and practice. Phytopathology 101:1024–1031. https://doi.org/10.1094/PHYTO-08-10-0216

Xu XM, Jeffries P, Pautasso M, Jeger MJ (2011b) A numerical study of combined use of two biocontrol agents with different biocontrol mechanisms in controlling foliar pathogens. Phytopathology 101:1032–1044. https://doi.org/10.1094/PHYTO-10-10-0267

Yaderets VV, Karpova NV, Glagoleva EV, Ovchinnikov AI, Petrova KS, Dzhavakhiya VV (2021) Inhibition of the growth and development of *Sclerotinia sclerotiorum* (Lib.) de Bary by combining azoxystrobin, *Penicillium chrysogenum* VKM F-4876d, and *Bacillus* strains. Agronomy 11:2520. https://www.mdpi.com/2073-4395/11/12/2520

Yan JT, Qiao K, Cai YF (2022) Application of *rpoB*, *gyrA* and *cheA* genes in identifying *Bacillus* genus. Acta Agriculturae Zhejiangensis 34:128–140. https://doi.org/10.3969/j.issn.1004-1524.2022.01.16

Yang CQ, Yu ZL, Yang J, Lei MY, Quan J, Yang TJ, Song XH (2020) Ecological actors and control strategies of root rot of *Coptis chinensis* in Shizhu County, Chongqing city. Plant Prot 46:160–166. https://doi.org/10.16688/j.zwbh.2019332

Yi YJ, Hou ZP, Yang Q, Cui LQ, Lu H, Li RF, Liu Y, Zhang YQ, Chen Y (2023) Antimicrobial mechanism and biocontrol effect of Bacillus cereus XZ30-2 on Aspergillus Niger. Qual Assur Saf Crops Foods 15:77–88. https://doi.org/10.15586/qas.v15i4.1379

Zhang D, Gao F, Jakovli I, Zou H, Wang GT (2020) PhyloSuite: an integrated and scalable desktop platform for streamlined molecular sequence data management and evolutionary phylogenetics studies. Mol Ecol Resour 20:348–355. https://doi.org/10.1111/1755-0998.13096

Zhao HH, Wang XB, Wang W (2022) *Bacillus amyloliquefaciens* SN16-1-induced resistance system of the tomato against *Rhizoctonia solani*. Pathogens 11:35. https://doi.org/10.3390/pathogens11010035

Zin NA, Badaluddin NA (2020) Biological functions of *Trichoderma* spp. for agriculture applications. Annals Agricultural Sci 65:168–178. https://doi.org/10.1016/j.aoas.2020.09.003

Publisher's Note Springer Nature remains neutral with regard to jurisdictional claims in published maps and institutional affiliations.